J Mol Model (2006) 12: 823–828
DOI 10.1007/s00894-006-0104-4

ORIGINAL PAPER

Balázs Jójárt · Árpád Márki

Comparative study of eight oxytocin antagonists by simulated annealing

Received: 20 October 2005 / Accepted: 15 December 2005 / Published online: 7 March 2006

Abstract In this study, eight oxytocin (OT) antagonists were subjected to conformational analysis. By means of simulated annealing, 2,000 structures were generated to sample the conformational space. The preferred main-chain and side-chain dihedral angles, intramolecular H-bond interactions (types 1←4 and 1←3), and secondary-structure elements (β-turns) were determined in the series of compounds. The influence of the modified amino acid on these structural elements was established; the values determined will be used as filtration criterion in preliminary research.

Keywords Peptide oxytocin antagonist · Atosiban · Conformational analysis · Simulated annealing

Abbreviations OT: Oxytocin · OTR: Oxytocin receptor · Mpa: β-Mercaptopropionic acid · dcpa: d-chlorophenylalanine · digl: d-indanylglycine · dpff: d-pentafluorophenylalanine · dtrp: d-tryptophan · ratc: 2R-2-Amino-2-carboxy-1,2,3,4-Tetrahydronaphthalene · rrmetcc: 1R,3R-1,2,3,4-Tetrahydro-1-methyl-β-carboline-3-carboxylic acid · rtcc: 3R-1,2,3,4-Tetrahydro-β-carboline-3-carboxylic acid · K_i: Inhibition constant

Introduction

Premature labor (parturition before 37 completed gestation weeks) is currently one of the greatest challenges in obstetrical practice. Besides the traditionally used β_2-sympathomimetics, which are associated with significant maternal and fetal side effects, there is a real need for more effective and more tolerable tocolytics. Although the causes of preterm labor are multifactorial, it is becoming increasingly apparent that oxytocin (OT) has an important role in preterm labor. It is accepted that both OT itself and the sensitivity of the uterus to OT play crucial roles in the initiation of both normal and pathologically early deliveries [1, 2]. Blockade of the uterine OT receptor (OTR) is one of the logical approaches to the prevention of preterm labor. Over the past decade, a number of potent OTR peptide and nonpeptide antagonists have been developed and studied in animal models. Atosiban ([Mpa^1,d-Tyr(OEt)^2,Thr^4,Orn^8] OT, Tractocile) is the first OT antagonist to be licensed for the treatment of preterm labor [3].

On the basis of the pharmacological characterization, we can summarize the structure-activity relationship of the peptides as follows: (1) the incorporation of Sar at position 7 leads to high antioxytocic and suppressed antidiuretic activities [4]; (2) peptides containing a basic amino acid (Arg or Orn) at position 8 are more potent [5]; (3) the amino acid at position 2 plays a key role in the antagonistic effect of the peptides: insertion of a d-amino acid at position 2 results in enhanced antioxytocic properties, and the antagonist potency can be increased further by an insertion of a bulky lipophilic amino acid at this position [6, 7]; (4) as neurohypophyseal hormones lacking an N-terminal amino group are inactivated quite slowly, most of the OT antagonists described to date contain Mpa (β-mercaptopropionic acid), Mca (β-mercapto-β,β-cyclopentamethylenepropionic acid), or Pen (β'-dimethylcysteine) instead of Cys at position 1 [8].

In this study, we made an attempt to determine the influence of the modified d-amino acid at position 2 on the structural elements of seven OT antagonists ([Mpa^1,Xxx^2,Gln^4,Sar^7,Arg^8]OT) [9], and to compare these elements with atosiban (**d(oet)tyr**). The modified d-amino acids at position 2 were as follows: d-4-chlorophenylalanine (**dcp**), d-indanylglycine (**digl**), d-pentafluorophenylalanine (**dpff**), d-tryptophan (**dtrp**), 2R-2-amino-2-carboxy-1,2,3,4-tetrahydronaphthalene (**ratc**), 1R,3R-1,2,3,4-tetrahydro-1-methyl-β-carboline-3-carboxylic acid (**rrmetcc**), and 3R-1,2,3,4-tetrahydro-β-carboline-3-carboxylic acid (**rtcc**) (Fig. 1).

B. Jójárt (✉) · Á. Márki
Department of Pharmacodynamics and Biopharmacy,
University of Szeged, Eötvös u. 6.,
Szeged 6720, Hungary
e-mail: jojartb@pharm.u-szeged.hu
Tel.: +36-62-545567
Fax: +36-62-545567

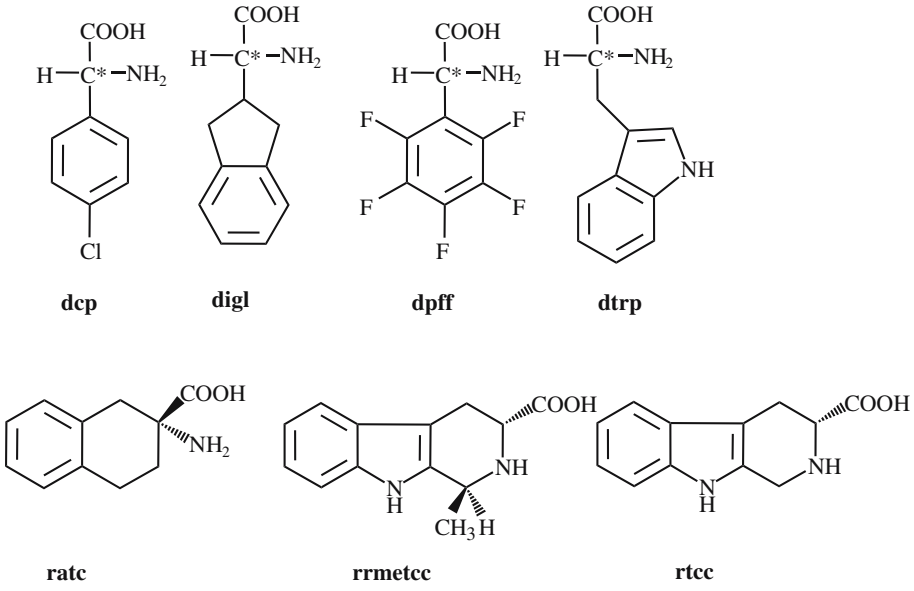

Fig. 1 Structures of the amino acids incorporated at position 2 in the ([Mpa[1],Xxx[2],Gln[4],Sar[7],Arg[8]]OT) OT antagonists

The inhibition constants (K_i) of the compounds tested were measured on the guinea-pig OTR, using [^{3}H]OT in heterologue displacement analysis (Table 1).

The amino acid sequence of the guinea-pig OTR is not yet available, and therefore we could not perform receptor-based comparative modeling of the peptides, and could not determine the bioactive conformation. The major aim of the study was to determine the structural differences in the peptides due to the conformational restricted amino acid at position 2.

Materials and methods

To explore the conformational space of the peptides investigated, simulated annealing was performed: (1) 2,000 structures were generated at high temperature (900 K); (2) the structures were minimized (grad=1) to avoid strained structures; (3) after the minimization, the structures were heated to 1,000 K (10 ps), equilibrated at 1,000 K (20 ps), and cooled down to 50 K (15 ps). After cooling, a final minimization was performed with the help of the steepest-descent, the conjugated-gradient, and finally the truncated-Newton methods in a consecutive manner; the gradients were 100, 10 and 0.001, respectively. The MMFF94s force field [10] with distance-dependent dielectric function (ε_r=4r) and no cutoff for the long-range nonbonding interactions was used. During the dynamic phase, the dihedral angles ω were restrained in the *trans* conformation.

All calculations were performed on dual AMD Opteron processors, running the Debian GNU/Linux 3.1 (Sarge) amd64 version, using the Molecular Operating Environment 2005.06 [11] software.

Table 1 The measured K_i values of the peptides investigated

	K_i±SEM (nM)
d(oet)tyr	5.76±1.48
dcp	9.00±2.00
digl	3.81±0.18
dpff	52.90±20.5
dtrp	37.60±23.2
ratc	1917.00±1682
rrmetcc	4700.00±745
rtcc	692.80±157

The radioligand binding assays were performed on pregnant guinea pig uterus membrane preparation, using [^{3}H]OT [9]

Results

Backbone dihedral-angle density plots (Φ^2–Ψ^2)

The first goal of the study was to detect the influence of the second, modified amino acid on the Φ–Ψ space distribution. Instead of the conventional Ramachandran plot, the more informative Ramachandran density plots were used. The Φ–Ψ space was divided into 20×20° boxes, and the number of structures in each box was calculated. Each resulting number was divided by the total number of conformers, providing the Ramachandran density normalized to unity. Only the density plots of the Φ^2–Ψ^2 space are depicted in Fig. 2 because alterations in the density are captured only in this space.

The density plots of the **d(oet)tyr**, **dcp**, **dpff**, **digl**, and **dtrp** compounds are very similar (Fig. 2a–e). The highest population was determined in the conformational space $-80° \le \Phi^2 \le -60°$ and $-40° \le \Psi^2 \le -20°$ for **d(oet)tyr**, **dcp** and **dpff,** and in the space $140° \le \Phi^2 \le 160°$ and $-160° \le \Psi^2 \le -140°$ for **digl** and **dtrp**. In each case, a major population was also found in the space $140° \le \Phi^2 \le 160°$ and $-160° \le \Psi^2 \le -140°$ (**d(oet)tyr**, **dcp** and **dpff**), and the space $-80° \le \Phi^2 \le -60°$ and $-40° \le \Psi^2 \le -20°$ (**digl** and **dtrp**). The sum of the densities in the five highest loaded spaces

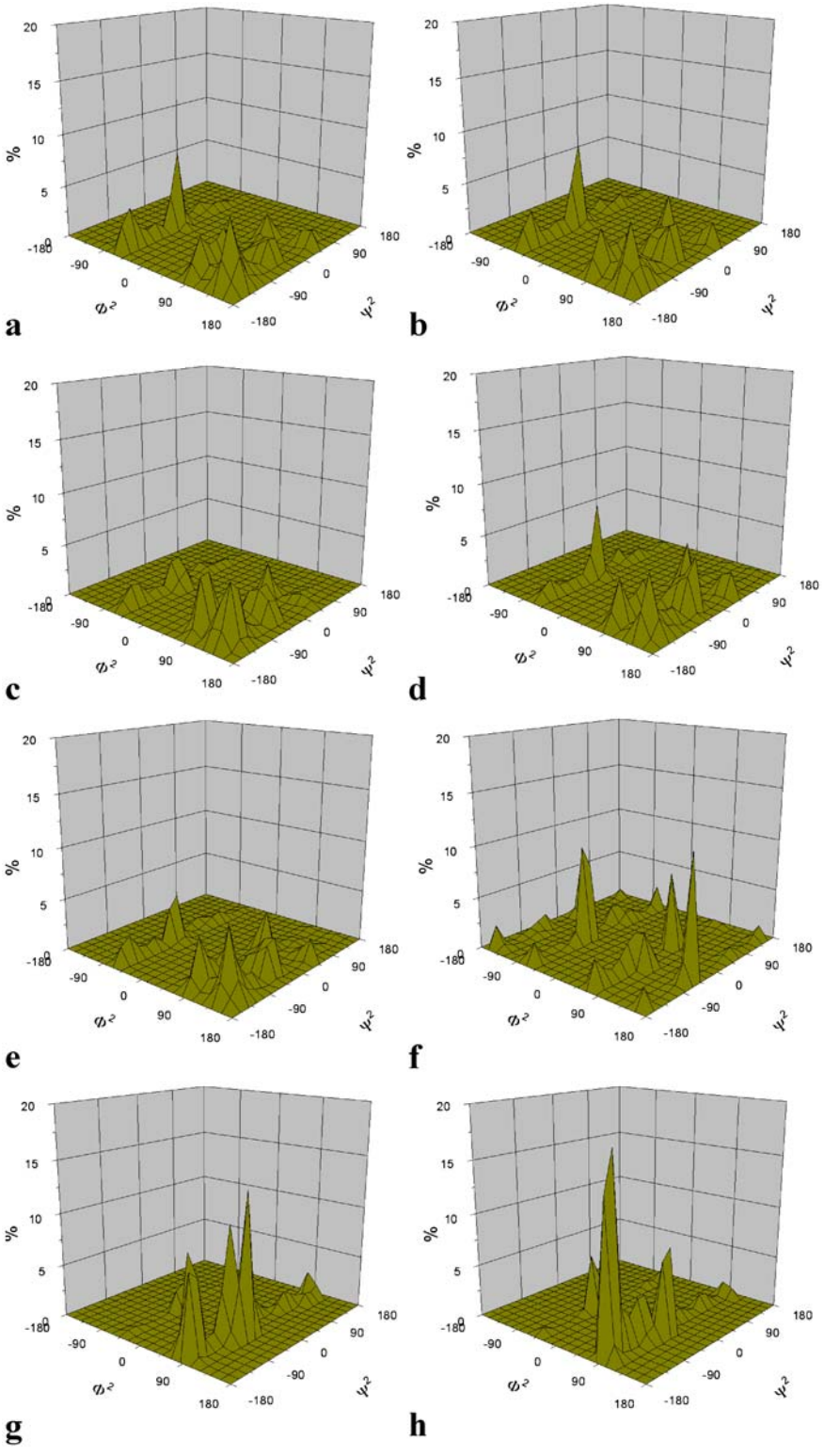

Fig. 2 Density distributions of the structures in Φ^2–Ψ^2 space: **d(oet)tyr** (**a**), **dcp** (**b**), **digl** (**c**), **dpff** (**d**), **dtrp** (**e**), **ratc** (**f**), **rrmetcc** (**g**), **rtcc** (**h**)

were 24.25, 25.75, 26.20, 23.85, and 23.15% for the **d(oet)tyr**, **dcp**, **dpff**, **digl**, and **dtrp** analogues, respectively.

In contrast, absolutely different density distributions were found in the remainder of the molecules. In the cases of **rrmetcc** and **rtcc** (Fig. 2g,h), the sum of the densities in the five highest loaded spaces was 47.05 and 43.45%, respectively. The highest population was determined in the space $100° \leq \Phi^2 \leq 120°$ and $-60° \leq \Psi^2 \leq -40°$ for **rrmetcc**, and the space $80° \leq \Phi^2 \leq 100°$ and $-160° \leq \Psi^2 \leq -140$ for the **rtcc** analogue.

For the **ratc** compound (Fig. 2f), the sum of the densities in the five highest loaded spaces was 41.15%, and the highest population was determined in the space $160° \leq \Phi^2 \leq 180°$ and $-60° \leq \Psi^2 \leq -40°$.

Table 2 χ^2 side-chain rotamer populations of the peptides investigated

a	g(+)(%)	g(−)(%)	+160°(%)	Σ
d(oet)tyr	40.00	18.45	39.60	98.05
dcp	41.50	21.70	35.20	98.40
digl	29.35	28.05	22.65	80.05
dpff	41.45	24.20	32.10	97.75
dtrp	37.50	23.85	36.40	97.75
b	−40°(%)	+30°(%)	160°(%)	Σ
rrmetcc	72.70	27.10	–	99.80
rtcc	84.75	15.25	–	100.00
c	+70°(%)	g(−)(%)	160°(%)	Σ
ratc	36.25	–	51.40	87.65

Side-chain conformation

The preferred orientations and the populations of the side chains were determined for all compounds. The influence of the modified amino acid at position 2 was found only in the χ^2 angle space, and therefore only this angle distribution is shown in Table 2a–c. Only a ±10° deviation was allowed from the values of the preferred orientation.

The analogues were also divided into three groups on the basis of the distribution of the side-chain populations. In the first group, containing **d(oet)tyr**, **dcp**, **digl**, **dpff** and **dtrp** (Table 2a), the preferred orientations were g(+), g(−) and +160°; among these orientations, g(+) and the +160° exhibited the largest rotamer populations.

In the second group, which contained the **rrmetcc** and **rtcc** molecules (Table 2b), only two preferred orientations were found, the −40° and +30° rotamers; the highly preferred orientation is that at −40° (72.70 and 84.75% for **rrmetcc** and **rtcc**, respectively).

For the **ratc** compound, two preferred orientations were again determined (Table 2c), the most preferred region being +160° (51.40%).

H-bond interactions

Three types of H-bond interactions were determined in the series of peptides: side-chain–side–chain, main-chain–side–chain, and main-chain–main-chain interactions. We accepted the electrostatic interaction as an H–bond when the distance between the acceptor and the H atom was less than 2.8 Å, and the angle formed by the acceptor, H and donor atom was higher than 90° [12].

In the case of the side-chain–side-chain interactions, only 8–9% of the 2,000 structures were found to be H-bonds. Among these structures, for atosiban the Thr^4-OG1···H–ND2Asn^5, and Asn^5OD1···H–NEOrn^8 type H-bonds were favored, whereas in the remaining compounds the Asn^5OD1···H –NE2Gln^4 type H-bond was the most preferred.

Three types of main-chain–side-chain H-bond interaction were also detected in all compounds: Asn^5OD1···HN–$NCys^6$ (16–19%), Gln^4O(Thr^4O)···H–ND2Asn^5 (5–7%), and Asn^5O···H–ND2Asn^5 (5–6%).

Main-chain–main-chain H-bonds were obtained as the most preferred electrostatic interaction. In Table 3, only those H-bonds are shown for which the occurrence was close to or more than 10%.

In the 1←4 H-bond interactions, Mpa^1O···HNGln^4/Thr^4 was most preferred; the remaining interactions were of the 1←3 H-bond type (Fig. 3).

Secondary structures

Although the secondary-structure elements are restricted by the ring structure of the OT analogues, we determined the possible β-turns of the peptides. We applied distance [d (C_i···C_{i+3}≤7 Å)] [13] and H-bond (regular H-bond between the O_i···HN_{i+3}) filters to determine the possible β-turn structures in six regions formed by residues 1–4 (region I), 2–5 (region II), 3–6 (region III), 4–8 (region IV), 5–8 (region V), and 6–9 (region VI) (Table 4).

In region II, region III, and region IV, a 40–44, 24–26 and 4–5% β-turn population was found, respectively. In region V there was a decreased, and in region VI an increased population of β-turns in all cases according to **d(oet)tyr**. In region I, a major population was found for the **ratc**, **rrmetcc**, and **rtcc** analogues as compared with **d(oet)tyr**.

The β-turn structures of the **ratc**, **rrmetcc**, and **rtcc** analogues are shown in Fig. 4.

Table 3 Percentage occurrences of main-chain–main-chain H-bonds in the peptides investigated

Acceptor	Mpa^1(O)		Xxx^2(O)	Ile^3(O)	Gln^4/Thr^4(O)	Cys^6(O)	Sar^7/Pro^7(O)
Donor	Ile^3(HN)	Gln^4/Thr^4(HN)	Gln^4/Thr^4(HN)	Asn^5(HN)	Cys^6HN	Arg^8/Orn^8(HN)	Gly^9(HN)
d(oet)tyr	9.90	4.65	11.45	15.25	10.00	14.65	9.40
dcp	10.00	5.40	11.35	16.35	9.85	13.90	11.75
digl	9.75	4.90	11.45	12.30	10.15	14.75	10.65
dpff	10.15	5.05	12.20	17.20	9.85	14.00	11.45
dtrp	9.40	4.80	12.60	15.15	9.75	13.45	11.25
ratc	17.20	8.80	11.70	13.45	11.30	13.50	9.45
rrmetcc	40.15	11.25	10.55	11.35	10.85	15.25	10.85
rtcc	18.75	7.95	11.20	12.15	12.15	14.15	9.70

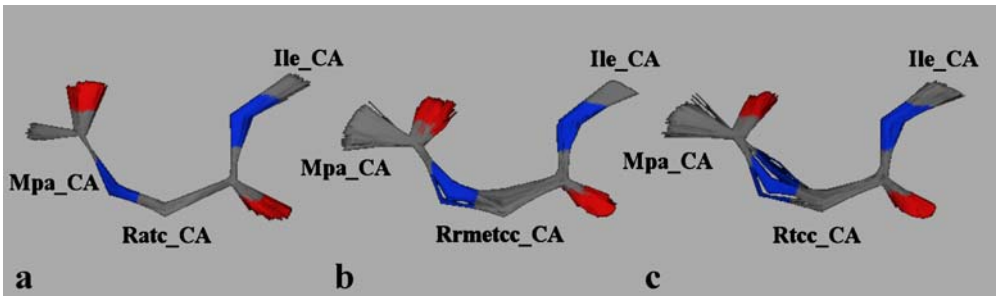

Fig. 3 The structures stabilized by 1←3 H-bond interactions for **ratc** (**a**), **rrmetcc** (**b**), **rttc** (**c**)

Table 4 Percentage occurrences of the β-turn structures in the various regions. Mpa[1]–Gln[4](Thr[4]) residues compose region I, Asn[5]–Arg[8](Orn[8]) residues region V, and Cys[6]–Gly[9] residues region VI

	Region I		Region V		Region VI	
	Distance	H-bond	Distance	H-bond	Distance	H-bond
d(oet)tyr	51.70	8.99	2.60	13.46	33.25	24.36
dcp	50.10	10.78	15.35	7.49	22.85	18.60
digl	49.05	11.42	19.70	9.14	21.35	22.95
dpff	47.90	10.54	13.95	7.89	21.45	18.88
dtrp	53.60	8.86	20.90	7.66	22.40	22.10
ratc	57.90	15.20	14.55	8.93	23.35	20.13
rrmetcc	57.25	19.74	19.75	9.11	22.70	23.13
rtcc	57.35	13.95	11.95	10.04	20.10	18.41

The first column lists the percentage occurrences of the β-turn structures in the various regions, using only the $\alpha(C_i \cdots C_{i+3})$ distance filter; the second column gives the percentage occurrences of structures stabilized by H-bonds

Discussion

In the course of the comparative structural analysis of the eight OT antagonists investigated, the consequences of the rigid amino acid at position 2 were established as concerns the main-chain and side-chain dihedral distributions, and also the H-bond interactions and secondary structure elements.

d(oet)tyr, **dcp**, **digl**, **dpff**, and **dtrp**, whose K_i values are less than 100 nM, exhibited very similar dihedral-angle distributions, H-bond interactions, and β-turn populations. The small alterations in the Ramachandran plots and in the χ^2 angle distribution of **digl** and **dtrp** should be explained by the very similar groups at position 2, whereas the remaining compounds contain phenylalanine derivatives in the cases of **d(oet)tyr**, **dcp**, and **dpff**.

In the remaining compounds, where a rigid structure arises because of the ring form of the amino acid at position 2, absolutely different structural elements were observed. For these compounds, more than 40% of the structures were found in five subregions of the Φ^2–Ψ^2 Ramachandran plots. These regions should be restricted areas in the case of a potent OT antagonist containing a d-amino acid at position 2. Further stabilizing effects are manifested in the 1←3 and 1←4 H-bond interactions, and also in the β-turn occurrence alterations in the cases of **ratc**, **rrmetcc**, and **rtcc**, where increased populations were obtained.

Summary

The goal of the study was to assign the structural differences in eight OT analogues containing bulky flexible or conformationally restricted amino acids. Two thousand structures were generated in the conformational sampling, and various structure elements, such as the main-chain and side-chain dihedral distributions, H-bond interactions, and secondary structures were determined. Differences were observed in the Φ^2–Ψ^2, χ^2 conformational space, in the occurrence of the main-chain–main-chain H-bond interactions (Mpa[1]CO···Ile[3]HN and Mpa[1]CO···Gln[4](Thr[4])HN) and in the β-turns (in ***region I***).

It is important to note that, when nonreceptor-based conformational sampling is used, determination of the bioactive conformation of a compound is very difficult. The results should be absolutely different from the bioactive conformation. A ligand containing a d-amino acid at position 2, possessing similar structural features to those of **ratc**, **rrmetcc**, and **rtcc**, might be excluded from the series of potent OT antagonists.

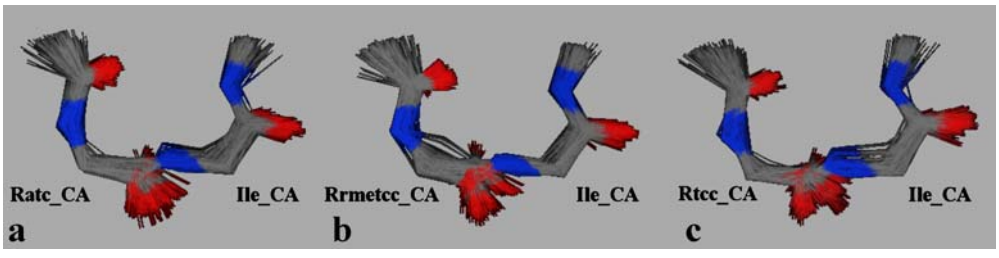

Fig. 4 The β-turn structures observed for **ratc** (**a**), **rrmetcc** (**b**), **rttc** (**c**)

Acknowledgement The help of András Mikó with the code in Perl used in the evaluation of the structures is gratefully acknowledged.

References

1. Fuchs AR, Fuchs F, Husslein P, Soloff MS, Fernstrom MJ (1982) Science 215:1396–1398
2. Takahashi K, Diammond F, Bieniarz J, Yen H, Burd L (1980) Am J Obstet Gynecol 136:774–779
3. Goodwin TM, Valenzuela G, Silver H, Hayashi R, Creasy GW, Lane R (1996) Am J Perinatol 13:143–146
4. Grzonka Z, Lammek B, Gazis D, Schwartz IL (1983) J Med Chem 26:1786–1787
5. Lebl M (1987) Analogs with inhibitory properties. In: Jost K, Lebl M, Brtnik F (eds) Handbook of neurohypophyseal hormone analogs, vol 2. CRC, Boca Raton, pp 17–74
6. Flouret G, Brieher W, Mahan K (1991) J Med Chem 34: 642–646
7. Melin P, Trojnar J, Johansson B, Vilhardt H, Akerlund M (1986) J Endocrinol 111:125–131
8. Grzonka Z, Kasprzykowski F, Lubkowska L, Darlak K, Hahn TA, Spatola AF (1991) Pept Res 4:270–274
9. Havass J, Bakos K, Márki Á, Gáspár R, Gera L, Stewart JM, Fülöp F, Tóth GK, Zupkó I, Falkay G (2002) Peptides 23:1419–1425
10. Halgren TA (1996) J Comput Chem 17:490–519, 520–552, 553–586, 587–615, 616–641
11. Molecular Operating Environment (MOE 2005.06) C.C.G. Inc, 1255 University St., Suite 1600, Montreal, Quebec, Canada
12. Aakeröy CA, Evans TA, Seddon KR, Pálinkó I (1999) New J Chem 23:145–152
13. Shclick T (2002) Molecular modeling and simulation—an interdisciplinary guide. In: Antman S, Marsden JE, Sirovich L, Wiggins S (ed) Interdisciplinary applied mathematics, vol 21. Springer, Berlin Heidelberg New York, pp 96–99